An IR Study of Hydrogen Bonding in Liquid and Supercritical Alcohols

Stephen J. Barlow,[†] Galina V. Bondarenko,[‡] Yuri E. Gorbaty,*[,‡] Toshio Yamaguchi,[§] and Martyn Poliakoff [†,||]

School of Chemistry, University of Nottingham, University Park, Nottingham, U.K. NG7 2RD, Institute of Experimental Mineralogy, Russian Academy of Sciences, Chernogolovka, Moscow Region, 142432 Russia, and Department of Chemistry, Faculty of Science, Fukuoka University, Fukuoka 814-80, Japan

Received: September 13, 2001; In Final Form: April 19, 2002

IR spectra in the region of the OH stretching band of liquid-like and supercritical methanol (T_c = 239.4 °C, P_c = 80.8 bar), ethanol (240.9 °C, 61.4 bar), 2-propanol (235.2 °C, 47.6 bar), and 1-butanol (289.9 °C, 44.1 bar) (data from ref 1, *J. Chem. Eng. Data* **1995**, *40*, 1025) have been recorded over a wide range of temperature and pressure up to 450 °C and 1000 bar. The spectra were obtained using a high-pressure, high-temperature IR cell and a specially developed measuring technique, in which the integrated intensity of the absorption band of the C−H stretching vibrations is used as an internal standard. This analysis allows the fraction of hydrogen-bonded and non-hydrogen-bonded hydroxyl groups in 2-propanol and 1-butanol to be estimated over the whole range of experimental conditions as a function of both temperature and pressure. With this approach, it is unnecessary to know the density of the sample or even the path length at which the spectra were obtained. However, the approach is less reliable in the case of ethanol and cannot be applied to methanol because the spectra of these substances are complicated by rotational fine structure. An unexpected result of this study is the possibility that only one type of hydrogen-bonded species exists in ethanol, 2-propanol, and 1-butanol when the mole fraction of hydrogen-bonded molecules is less than about 0.6. When the probability of hydrogen bonding is greater, evidence for a strong cooperative effect is seen.

1. Introduction

Supercritical (sc) fluid technologies have opened up new opportunities in many areas of chemistry and engineering but so far it has been supercritical CO_2 and to a lesser degree supercritical water, scH_2O, that have attracted most attention.[2] It has been demonstrated that $scCO_2$ is an effective medium for a wide variety of chemical reactions and processing,[3] whereas oxidation in scH_2O has been shown to be highly efficient.[4] A large driving force for the application of these fluids has been the environmental benefits they provide compared to conventional solvents, coupled with the ability to optimize the characteristics of the fluid by adjusting the temperature and pressure. The use of other sc fluids, such as sc alcohols and $scNH_3$ has been less widespread, despite being much less aggressive than scH_2O and having lower critical parameters. Nevertheless, supercritical methanol (MeOH), ethanol (EtOH), and 2-propanol (^{i}PrOH) have found applications mainly in the preparation of solid-state materials,[5−7] as well as in polymer recycling[8] and transesterification.[9] In addition, it has been shown that sc^{i}PrOH can enable transfer hydrogenation reactions to take place without the need for either hydrogen or a catalyst.[10]

The nature of H-bonded substances, such as simple alcohols, has attracted interest for the majority of the last century.[11] H-bonded chain structures are believed to predominate in the liquid states of a number of alcohols, particularly in MeOH and EtOH, which have been studied extensively. Evidence for these structures includes information from computer simulations,[12−17] molecular dynamics (MD) analysis of ^{1}H NMR data,[18] and X-ray diffraction.[19,20] In contrast, detailed analyses of the *same* diffraction data have found clusters of different types[21,22] or have been inconclusive.[23] More recent neutron diffraction studies have attempted to clear up these ambiguities, again suggesting the formation of winding chainlike structures.[24−26] Further X-ray and neutron diffraction experiments have investigated the effect of pressure on liquid MeOH.[27] In addition, liquid *tert*-butyl alcohol has been subject to a number of recent studies,[28,29] including a combined MD and ^{1}H NMR investigation by Yonker et al., which suggested the prevalence of a cyclic tetramer.[30]

The importance of understanding the nature of intermolecular interactions, such as hydrogen bonding, in sc fluids has been recognized for some time.[31−33] For example, it has been suggested[34] that the unusual properties of H_2O arise from its peculiar physical state, which in turn depends on the connectivity of a network of H-bonded molecules. The question of the degree of hydrogen bonding found in scH_2O and its structure has attracted considerable interest over the past decade.[34−37] The effect of pressure and temperature on the ^{1}H NMR spectrum of MeOH has been studied quite extensively.[38−42] Hoffmann and Conradi[38] measured the chemical shift of the hydroxyl proton of MeOH and EtOH up to 450 °C and 400 bar. Comparing this shift relative to that of the CH_3 resonance, they estimated the degree of hydrogen bonding using a simple model. MD simulations[40,43] have suggested that the structure is made up of long chains, which are broken into shorter chains at lower densities. Most recently, Yamaguchi et al.[44] completed a neutron diffraction study which, in contrast to the MD simulations, suggested that clusters of 3−5 molecules exist at moderate densities in scMeOH.

The use of IR spectroscopy in the study of H-bonded systems has a long history. There have been many experimental studies

[†] University of Nottingham.
[‡] Russian Academy of Sciences. E-mail: hunch@issp.ac.ru.
[§] Fukuoka University. E-mail: yamaguch@sunsp1.sc.fukuoka-u.ac.jp.
[||] E-mail: Martyn.Poliakoff@nottingham.ac.uk. http://www.nottingham.ac.uk/supercritical/.

10.1021/jp0135095 CCC: $22.00
Published on Web 09/28/2002

of hydrogen bond associations in alcohols under various conditions and in solution.[45−49] More recently, the development of new IR techniques has begun to give a further understanding of the topology of H-bonded clusters in alcohols[50−54] and the use of IR in the study of associations in MeOH has been recently reviewed.[55] Obtaining spectra of pure liquid alcohols in the mid-IR region is often complicated by the need to use very short path lengths, a situation made even more difficult at high temperature and pressure. Perhaps this is the reason, to the best of our knowledge, there have not been many previous studies of alcohols in the mid-IR region at high temperatures. These difficulties may be circumvented either by investigating the NIR spectrum[56] or by turning to Raman spectroscopy, as in the work of Ebukuro et al.[57] on scMeOH. However, IR spectroscopy is generally more sensitive to hydrogen bonding.

Here we aim to estimate the degree or the probability of hydrogen bonding in a series of alcohols in a variety of thermodynamic states, using IR spectroscopy. We use the term "probability" only to emphasize the probabilistic character of the phenomenon of hydrogen bonding and the fact that our results are only semiquantitative estimates.

2. Experimental Section

MeOH ("Khimreactiv", 0.4% H_2O), EtOH, (Fisher, 0.2% H_2O), 2-propanol ("Khimreactiv", 0.3% H_2O) and 1-butanol (Fisher, 0.2% H_2O) were dried over molecular sieves and degassed prior to use. A unique high-pressure, high-temperature (HPHT) cell with sapphire windows has been used for quantitative measurement of IR or FTIR absorption spectra. The cell is essentially a modified and improved version of our earlier cell with a variable path length.[58] The ability to vary the path length of this cell *during an experiment* at high temperature and pressure allows one to circumvent most of the common and specific errors that distort the shape of absorption bands and affect the accuracy of intensity measurements. Common sources of error include contributions from atmospheric water vapor and CO_2, scattering of light within a sample, limited and uneven transparency of windows, and light losses at reflections. The most serious specific source of error, which is of greater concern for dispersive spectrometers, is the vignetting of the beam because of the insufficient linear and angular apertures of HPHT cells. All these errors are avoided by recording the spectrum as a difference between two absorbance spectra obtained at different path lengths under otherwise identical conditions. For accurate quantitative measurements, one only needs to know the difference between the path lengths, which can be found using a micrometric microscope or a precision transducer. However, there is no need to know the absolute path lengths in the particular experiments described here. It is only necessary that both path lengths should provide absorbances in the range of approximately 0.3−1.1 for both ν_s(O−H) and ν_s(C−H). Typically, the absolute path lengths *used in this work* were in the range 60−150 μm, and the difference Δ between them varied from ca. 4 to 100 μm.

The cell consists of two main parts: the cell itself and a drive mechanism, which reduces the force needed to change the path length. The latter moves the body of the cell relative to one of the windows fixed to the pillar of the drive mechanism. The cell has a movable thermocouple, which is very useful to calibrate the thermocouple in the normal position, that is, outside the irradiated volume. In this study the transverse temperature gradient did not exceed 2−3 °C even at the highest temperatures and low pressures and was less than 1 °C for denser states. The cell can withstand conditions as severe as 500−550 °C at 1500 bar and can be used both in static and flow modes. Naturally, the cell can be used also as a fixed path length cell if necessary. One can simply put gaskets between windows and press them together. However, using a fixed path length over a large range of densities and temperatures to study OH absorptions is very inconvenient.

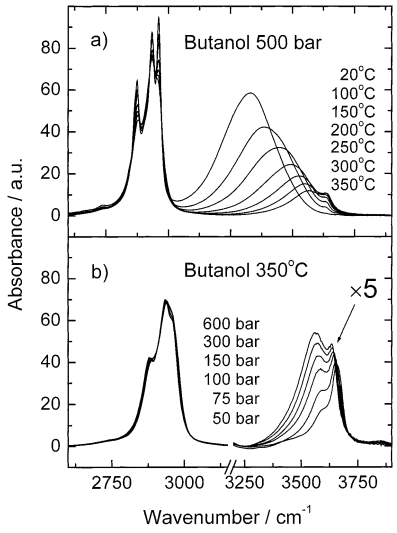

Figure 1. (a) Normalized spectra of 1-butanol at isobaric heating in the region of the C−H and O−H stretching vibrations. (b) Same for isothermal compression. The intensity in the region of ν_s(O−H) is expanded by a factor of 5.

Two such cells differing only in the window diameter (12 and 10 mm) were simultaneously put to use, the 12 mm windowed cell with a ratio-recording IR spectrophotometer Perkin-Elmer 983 (at IEM RAS) and the other with a FTIR interferometer Perkin-Elmer 2000 (at the University of Nottingham). All spectra were recorded with a resolution of 4 cm^{-1}. However, no difference was found between the results obtained with these two experimental setups, except, of course, that FTIR is certainly faster, more convenient, and precise. The data on MeOH and ^{i}PrOH were obtained with the dispersive spectrometer, whereas data on EtOH and 1-butanol (^{n}BuOH) were recorded with FTIR. A detailed description of the earlier cell is given elsewhere.[58a]

3. Data Treatment

It is well-known that in the high-density liquid phase, the spectra of alcohols are dramatically different from those of gaseous phases with much broader spectra, shifted to lower wavenumbers due to increased hydrogen bonding and frequency of collisions between molecules. In this study, we examine the IR spectra at a range of intermediate and high densities and implement the procedure described below to estimate how H-bonding varies under different conditions.

Our procedure for data processing can be illustrated by analysis of the spectra of ^{n}BuOH. Figure 1 shows the spectra in the region of the ν_s(O−H) stretching vibrational modes obtained at a constant pressure of 500 bar (Figure 1a) and at isothermal compression (Figure 1b). As can be seen, heating of the sample or a decrease in density leads to a strong decrease in the peak intensity and a shift to higher frequencies. Simultaneously, the intensity of a relatively narrow band, corresponding to monomeric (i.e., non-H-bonded) hydroxyl groups, increases, whereas its position changes slightly between approximately 3635 and 3640 cm^{-1} (cf. 3671 cm^{-1} in the gas phase). It should be stressed that the band due to the monomeric

TABLE 1: Integrated Intensity of Absorption of ν_s(C−H) for Methanol and 2-Propanol

T, °C	P, bar	ρ, g cm^{-3}	Δ, micron	A_{C-H}, km mol^{-1}
		Methanol		
350	100	0.082	112	119.2
350	200	0.244	27	103.2
350	300	0.378	26	109.7
350	400	0.451	21	108.6
350	500	0.504	19	106.0
		2-Propanol		
200	500	0.687	3.2	152.8
250	500	0.619	4.0	149.7
300	500	0.581	4.6	157.0

species includes also a contribution from the "free OH" of hydrogen bond acceptor molecules at the terminus of linear multimers.[50,59] The resolution of this absorption band, even at high density and low temperature, is sufficient to apply a peak fitting procedure to evaluate the approximate fraction of non-H-bonded OH groups. Normally, to calculate the fractions of H-bonded and non-H-bonded molecules, the value of the absorption coefficient needs to be known but the density of ^{n}BuOH at high pressures and temperatures remains as yet unknown. To overcome this difficulty, we suggest an approach based on the assumption that over the range of experimental conditions, the coefficient of the integrated absorption

$$A = \int_{\nu_1}^{\nu_2} \kappa(\nu)\, d\nu \qquad (1)$$

where $\kappa(\nu)$ is the molar (Napierian) absorption coefficient, does not change significantly for all the bands corresponding to the ν_s(C−H) vibrations. Some indirect evidence in favor of this point is provided by the fact that the peak positions of ν_s(C−H) bands in the spectra of the four alcohols do not change over the whole range of temperature and pressure explored, at least within the limits of instrumental error (see corresponding spectral region in Figure 1a,b). This means that neither temperature nor density nor O−H···O hydrogen bonds affect the C−H configuration of the molecules noticeably. Table 1 shows the integrated intensity A of the ν_s(C−H) band for MeOH and ^{i}PrOH in the few cases for which we were able to find the density values. As can be seen, A remains constant within the limits of experimental error.

So, taking into account changing density, we may reduce the spectra obtained at different temperatures and pressures to the equal areas under the ν_s(C−H) bands, as shown in Figure 1a,b. The resulting normalized spectra of ^{n}BuOH in the ν(O−H) region obtained at a constant pressure of 500 bar are shown in Figure 1a, whereas Figure 1b demonstrates normalized O−H spectra at a constant temperature of 350 °C. Obviously, the units for the spectra processed in this way have the same meaning as for the molar absorption coefficient κ in eq 1 but they refer to an unknown *arbitrary "molecular unit"* instead of a mole.

The spectra in the region of the ν_s(O−H) modes can be assumed to be the sum of overlapping absorption bands of H-bonded and non-H-bonded OH groups. Indeed, we found that the spectra can be approximated well by three mixed Gaussian and Lorentzian functions. The question of the actual shape of the absorption bands is rather complicated. It is influenced, in particular, by the character of rotational movement in liquids, which depends on temperature and density. It is known that at high temperatures, as the diffusion limit (pure diffusional rotation) is achieved, the contour of a band is close to the Lorentzian, whereas at low temperature the band is described better by a Gaussian function. Figure 2 shows an example of

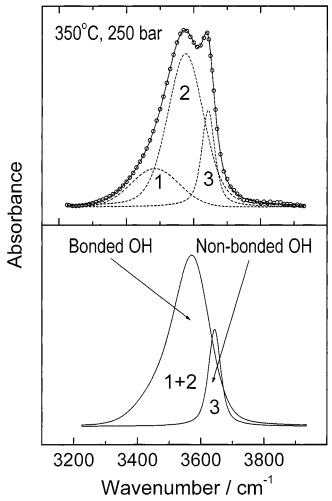

Figure 2. Example of the fitting procedure, shown for 1-butanol. (a, Top) experimental spectrum (circles), mixed Gaussian−Lorentzian functions (dashed lines), and their sum (continuous line). (b, Bottom) peak "1+2" is the sum of the first and second components of deconvolution (H-bonded OH), and peak "3" is the third component (non-H-bonded OH).

the fitting procedure for ^{n}BuOH. Two broad low-frequency functions represent the distribution of H-bonded OH groups, whereas the narrow high-frequency component is attributed to the monomeric OH groups. It should be stressed that, because we can see no specific features (shoulders, bending points) in the contour of the broad band corresponding to the H-bonded OH groups, we can only consider their distribution as a *continuum*. So, we place *no physical meaning* in the presentation of H-bonded molecules as a sum of two peaks (1 and 2). This is only to describe a slight asymmetry of the distribution. On the other hand, solutions of some alcohols in hexane[60] or CCl_4[61] show distinct evidence of multicomponent composition of the band of H-bonded OH. In such cases, advanced analysis is possible, such as, for example, Førland et al.[61] have performed.

If the spectral bands are not well resolved, fitting procedures must always be used very cautiously. In such cases, the problem may not have a unique solution. In fact, we could obtain as good a fit as that in Figure 2 with slightly different parameters of individual bands. However, to find the most consistent solution, we repeated the procedure several times with different initial parameters, with the aim of achieving not only the best fit but also more or less smooth trends for all the parameters of deconvolution (positions, widths, intensities, % of Lorentzian) over the whole experimental series, as shown in Figure 3. Only such an approach can provide reliable results.

Figure 4a shows the behavior of the integrated intensity of H-bonded (the sum of areas under peaks 1 and 2) and non-H-bonded OH groups (peak 3) during isothermal (350 °C) compression. The pressure trend of the integrated intensity of monomeric OH I_{nb} can be well approximated by an exponential function. Extrapolation of the function to zero pressure (which means to zero density) gives the *reduced* coefficient of integrated intensity A_{nb} for the monomeric OH groups in the same arbitrary units. It is then straightforward to extract the nondimensional fractions of H-bonded and non-H-bonded OH groups from their total intensities. The mole fraction of the non-H-bonded OH groups X_{nb} is equal to I_{nb}/A_{nb} and the mole fraction of the H-bonded OH groups is $X_b = (1 - X_{nb})$.

The coefficient A_{nb} is, of course, to some extent sensitive to the nearest environment, but this effect is incomparably less than the influence of H-bonding and, following literature

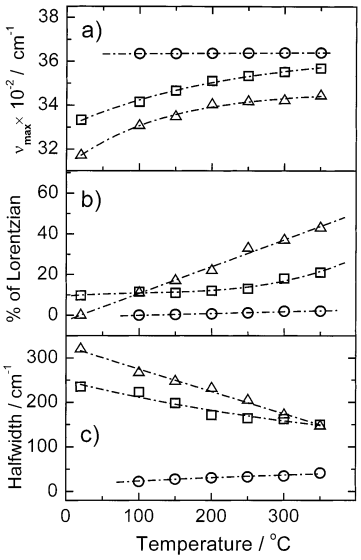

Figure 3. Parameters of deconvolution in the isobaric series (1-butanol, 500 bar): (a) peak positions; (b) percentage of Lorentzian; (b) half-widths. Key: (triangles) first component; (squares) second component; (circles) third component.

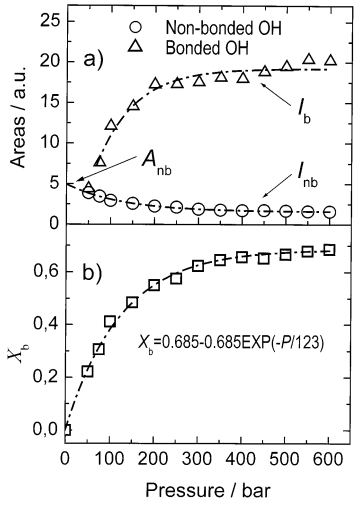

Figure 4. Determination of degree of hydrogen bonding in 1-butanol at a constant temperature of 350 °C: (a) pressure trends for the integrated intensities of H-bonded and non-H-bonded OH groups; (b) pressure trend for the mole fraction of H-bonded OH groups.

data,[60,62−64] can be assumed to be constant in the rough approximation used in this work.

Figure 4b shows the behavior of X_b during isothermal compression. It is easy to see that using such an approach, it is necessary to know neither the density nor the path length. The only mandatory condition is that I_{nb} and A_{nb} for all the spectra in the series must be expressed in the same arbitrary units. We have deliberately avoided listing the exact values of A_{nb} obtained with this procedure because they can have any arbitrary value. In most cases, we used absorbance spectra obtained simply as 1000 $\ln[T_2(\nu)/T_1(\nu)]$ (just to avoid bother over the decimal point), where $T_1(\nu)$ and $T_2(\nu)$ were two consecutive transmittance spectra at different path lengths. However, we could just as well have used any other factor instead of 1000.

It is clear that the accuracy of X_b determination depends first of all on the reliability of the fitting procedure, which in turn depends on the resolution of the stretching bands of H-bonded and non-H-bonded OH. If there is no resolution, the task becomes practically impossible. The better the resolution, the narrower is the range of possible solutions. To estimate the limits of uncertainty, we tried to change significantly the behavior of the parameters of deconvolution, to find further smooth trends with a reasonable fit. In this way we could estimate the accuracy of the X_b determination for ^{n}BuOH as $\pm 10-12\%$. The scatter for A_{nb} values is typically $\pm 5\%$.

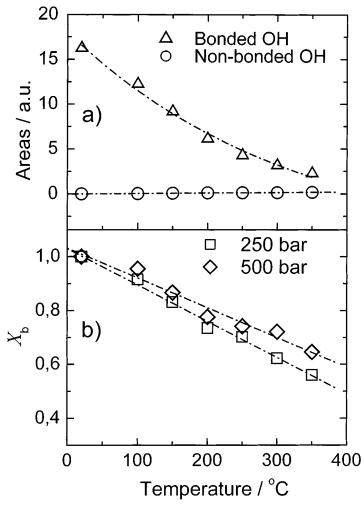

Figure 5. Determination of degree of hydrogen bonding in 1-butanol at isobaric heating: (a) temperature trends for the integrated intensities of H-bonded and non-H-bonded OH groups at a constant pressure of 500 bar; (b) temperature trends for the mole fraction of H-bonded OH groups at pressures 250 and 500 bar.

4. Results and Discussion

4.1. 1-Butanol. Spectra of ^{n}BuOH have been obtained along isotherm of 350 °C in the pressure range from 50 to 600 bar and along isobars 250 and 500 bar up to 450 °C. However, only the data obtained up to 350 °C were used in this work because the high-temperature spectra of all four alcohols have shown that slow decomposition occurs at a temperature of 450 °C. The decomposition, although less obvious, is still noticeable at 400 °C, but the alcohols seem quite stable at 350 °C. Decomposition products such as CO and CO_2 and any changes in the shape of the ν_s(C−H) bands could be conveniently monitored in situ using the IR absorption.

The effect of pressure on the extent of hydrogen bonding has already been shown in Figure 4b. The pressure trend can be well approximated by an exponential function. The limit of this function is about 0.68, which means that the probability of hydrogen bonding X_b at a temperature of 350 °C can never reach 1.

The strong effect of temperature on the behavior of the OH band at a constant pressure of 500 bar is seen in Figure 1b. To obtain the value of X_b as a function of temperature, the spectra were again normalized to the same arbitrary "standard" area under the ν_s(C−H) bands as in the isothermal series. This allows us to use the same value of the reduced coefficient of integrated absorption A_{nb}. The same fitting procedure, described above, was followed to find the integrated intensities of H-bonded and non-H-bonded species. Figure 5a demonstrates the behavior of the integrated intensities, that is, the areas under the fit components. The same procedures were applied to the spectra obtained at a constant pressure of 250 bar. Dividing I_{nb} by A_{nb}, we obtain X_{nb} and thus X_b. Figure 5b shows the final result of X_b determination for both isobars. The data appear quite reasonable. The mole fraction of H-bonded OH groups changes from 1 to approximately 0.6. It can be seen that the probability

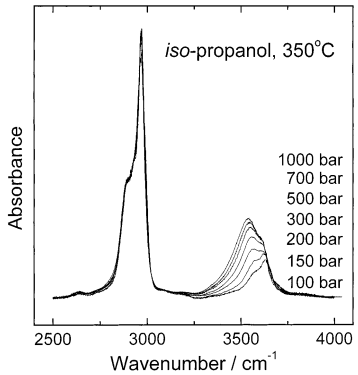

Figure 6. Normalized spectra of 2-propanol obtained at isothermal compression.

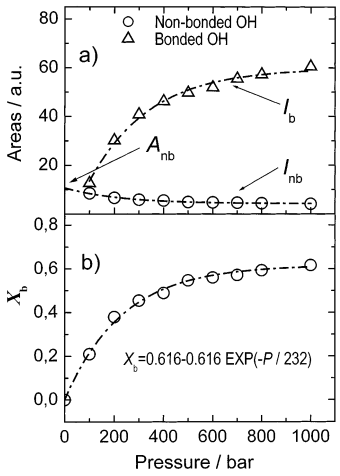

Figure 7. Determination of degree of hydrogen bonding in 2-propanol at a constant temperature of 350 °C: (a) pressure trends for the integrated intensities of H-bonded and non-H-bonded OH groups; (b) pressure trend for the mole fraction of H-bonded OH groups.

of hydrogen bonding at a pressure of 250 bar is lower than at higher pressure. In addition, the trend is approximately linear, as found for MeOH and EtOH using NMR under similar conditions.[38]

4.2. 2-Propanol. Spectra of ^{i}PrOH were obtained at a constant temperature of 350 °C in the pressure range from 100 to 1000 bar and along the isobars 500 and 1000 bar. Figure 6 shows some of the normalized spectra obtained under isothermal compression. It can be seen that the monomeric band in the spectra of ^{i}PrOH is not as well resolved as in the case of ^{n}BuOH. Nevertheless, it is still possible to use the fitting procedure to find the probable contribution of non-H-bonded OH groups to the spectra. The behavior of the integrated intensities of H-bonded and non-H-bonded species is shown in Figure 7a, whereas Figure 7b indicates the estimate of X_b at isothermal compression. The pressure trend of X_b for ^{i}PrOH is very similar to that for ^{n}BuOH (Figure 4b). Even the limit for the exponential function ($X_b = \sim 0.62$) is fairly close to that for ^{n}BuOH. Again, similar trends have been reported for EtOH and MeOH from ^{1}H NMR data.[38]

The effect of temperature on the probability of hydrogen bonding in ^{i}PrOH can be seen in Figure 8, where the integrated intensities for the isobar 1000 bar (Figure 8a) and X_b for the isobars 500 and 1000 (Figure 8b) bar are presented as functions of temperature. There is a small difference in the behavior of X_b as a function of temperature between ^{n}BuOH and ^{i}PrOH. In the latter case, a slight curvature is observed but the deviation from linearity is within the limits of probable error.

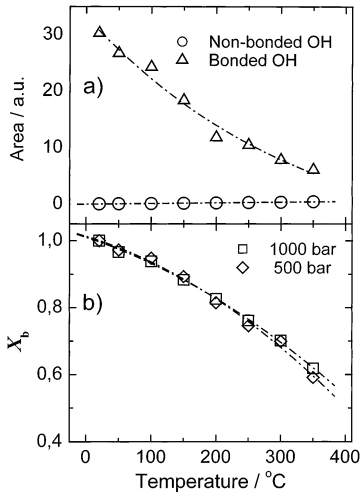

Figure 8. Determination of degree of hydrogen bonding in 2-propanol: (a) temperature trends for the integrated intensities of H-bonded and non-H-bonded OH groups at a constant pressure of 1000 bar; (b) temperature trends for the mole fraction of H-bonded OH groups at pressures 500 and 1000 bar.

4.3. Integrated Intensities for H-Bonded OH Groups in ^{n}BuOH and ^{i}PrOH. So far we have not considered the intensities of the H-bonded OH groups I_b obtained as the sum of areas under the first and the second components of deconvolution (see Figure 2). However, the coefficient of integrated absorption is a very sensitive characteristic of hydrogen bonding. The *reduced* coefficient of integrated absorption A_b can be found as $A_b = I_b/X_b$. It is interesting to see how the coefficient A_b correlates with the mole fraction of H-bonded OH groups. It is well-known that the coefficient increases strongly with the strength of hydrogen bonds.[65] In ice, for example, in which all possible hydrogen bonds are formed, the coefficient is ca. 25−30 times greater than for water vapor.[66,67]

As the amount of H-bonded OH groups increases, one ought to expect a monotonic growth of A_b. In fact, the situation is quite unexpected and very interesting. Parts a and c of Figure 9 demonstrate the correlation between the coefficient of integrated absorption A_b and the mole fraction X_b of H-bonded OH groups over the full range of the explored external conditions for ^{n}BuOH and ^{i}PrOH. One can see that it is possible to approximate the correlation by a function with a sharp bend at $X_b = 0.65 \pm 0.05$. To highlight this unusual behavior, each array of experimental points in Figure 9a−c is fitted by two linear functions. The reason for such a strange phenomenon may be that at X_b less than 0.6 (that is, at low density and high temperatures), a H-bonded species *of only one type* is in equilibrium with the monomer. The simplest explanation is that this aggregate is most likely to be a dimer, but direct evidence for this cannot be extracted from the data presented here. On the other hand, the approximate position of ν_{max} for the band representing H-bonded continuum in the supercritical region (ca. 3580 cm^{-1} for ^{n}BuOH and ca. 3560 cm^{-1} for ^{i}PrOH) are very close to known bands of dimers in the gas phase at room temperature (ca. 3560 cm^{-1} in ^{i}PrOH),[53,68] in a matrix at 35 K[45] (ca. 3525 cm[1]) and solutions of ethanol in hexane[69] (ca. 3540 cm^{-1}).

Given the uncertainty in the deconvolution procedure, we cannot be absolutely sure of this surprising result. However, the same conclusion can be made independently, using other spectroscopic data. Parts b and d of Figure 9 show the correlation between the maximum position ν_{max} of the band corresponding to the H-bonded OH groups and X_b for ^{n}BuOH and ^{i}PrOH,

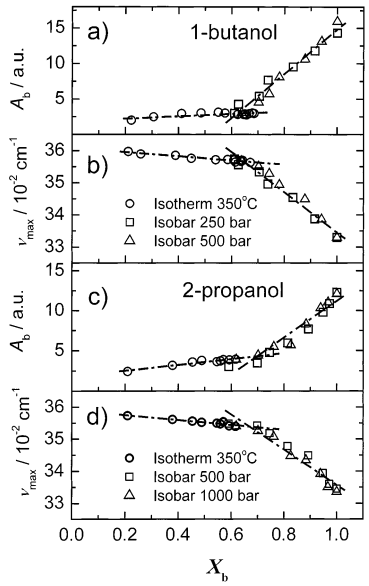

Figure 9. (a) Correlation between the coefficient of integrated absorption A_b and the mole fraction X_b of H-bonded OH groups for 1-butanol. (b) Correlation between peak positions of H-bonded OH groups for 1-butanol and (a) and X_b. (c) and (d) the same for 2-propanol.

respectively. Again we can distinguish a quite different behavior of ν_{max} below $X_b = \sim 0.6$ and above ~ 0.7. We obtain what seems like two mirror images in Figure 9a,b and 9c,d. This is not surprising because in the case of hydrogen bonding there is always a strong (and as a rule linear) correlation between the coefficient of integrated absorption and the position of the band. The correlation between ν_{max} and X_b is evidence that our estimate of A_b as a function of X_b is reasonable. Even the positions of the break points in the curves correspond closely. The sudden increase in the coefficient of integrated intensity at $X_b \approx 0.65$ could be explained by the onset of a cooperativity effect as multimolecular H-bonded species begin to form. The effect of cooperativity increases the average energy of bonding with every new molecule of alcohol added to a chain through O−H···O bonds. The effect is of primary significance for understanding the behavior of systems with hydrogen bonds and is especially important for biological systems. Using the theory developed by Veytsman,[70] Gupta and Brinkley[60] have shown indirectly that their spectroscopic data on pentanol and hexanol cannot be properly interpreted without taking into account the cooperativity effect of hydrogen bonding. Here we present direct evidence for this phenomenon.

Our data do not allow us to say definitely which particular polymer-like species exist above $X_b \approx 0.6-0.7$. There are speculations[71] that addition of the next OH group to the existing H-bonded complex can result not only in the strengthening of bonds but, in some cases, in their weakening. Indeed, if the bond is strongly bent, as in the case of small cyclic clusters, one may expect a decrease in the energy of hydrogen bonds.[72] Yukhnevich[73] analyzed a large number of spectroscopic data and found that both the proton-donor and proton-acceptor abilities of an XH group increase with the addition of each extra molecule. He also found that the angle of the H-bond influences the cooperativity effect. The fact that in our case the effect of cooperativity seems fairly strong allows us to assume that multimolecular H-bonded complexes are either chainlike or fairly large rings.

It seems highly likely that only a dimer is present in equilibrium with the monomer over the whole density range corresponding to the supercritical isotherm at 350 °C. Looking

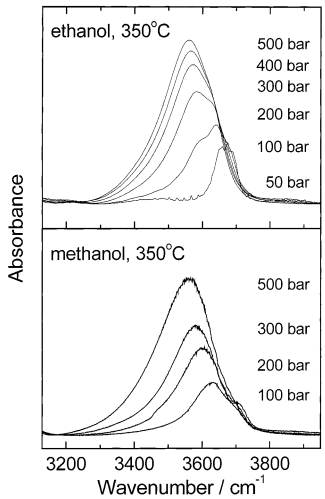

Figure 10. (a) Normalized spectra of EtOH at the isothermal compression. (b) Corresponding spectra for MeOH.

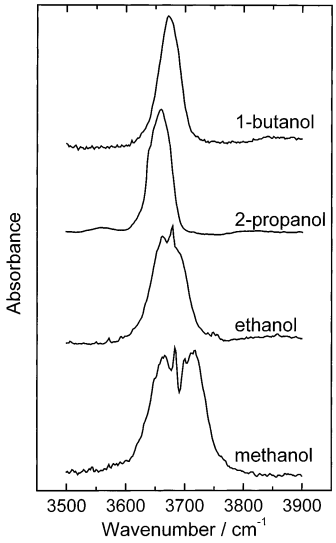

Figure 11. Spectra of gaseous MeOH, EtOH, ^{n}BuOH, and ^{i}PrOH in the region of OH stretching vibrations.[75]

at the temperature isobaric trends for ^{n}BuOH and ^{i}PrOH, it seems that dimers prevail in possible H-bonded species at all supercritical temperatures up to the temperature of decomposition.

4.4. Ethanol and Methanol. Spectra of EtOH and MeOH along the isotherm at 350 °C are shown in Figure 10. Again, it is possible to see a trend with decreasing pressure similar to that observed for the spectra of ^{n}BuOH and ^{i}PrOH. However, we are unable to apply exactly the same procedure to determine the probability of hydrogen bonding in EtOH and MeOH. The reason our methodology is successful for ^{n}BuOH and ^{i}PrOH but not EtOH and MeOH can be explained by comparing the spectra of all four alcohols in the gaseous state (Figure 11). It can be seen that the ν(O−H) bands of gaseous ^{n}BuOH and ^{i}PrOH can be more or less correctly presented as uniform single-peak distribution functions but the spectra of MeOH and EtOH are largely made up of the partially resolved P, Q, and R branches of the rotational transitions, with the Q branch centered between 3660 and 3690 cm^{-1}. Because of the smaller rotational constant of the large ^{i}PrOH molecule, the rotational branches are less pronounced. In the case of ^{n}BuOH the branches are practically absent. It is clear that at the lowest densities, the spectrum of EtOH at 50 bar and 350 °C is a typical rotation−vibration spectrum that cannot be fitted in the procedure of

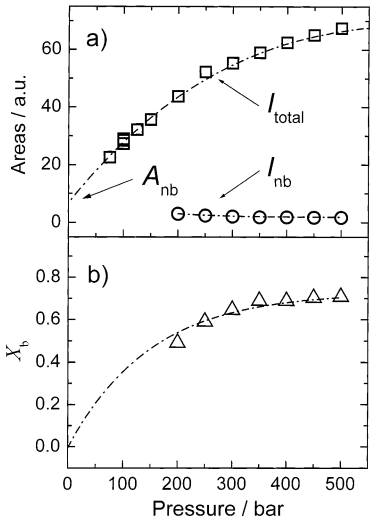

Figure 12. Degree of hydrogen bonding in EtOH at a constant temperature of 350 °C: (a) pressure trends for the total integrated intensity of OH band (squares) and for non-H-bonded OH groups (circles); (b) pressure trend for the mole fraction of H-bonded OH groups.

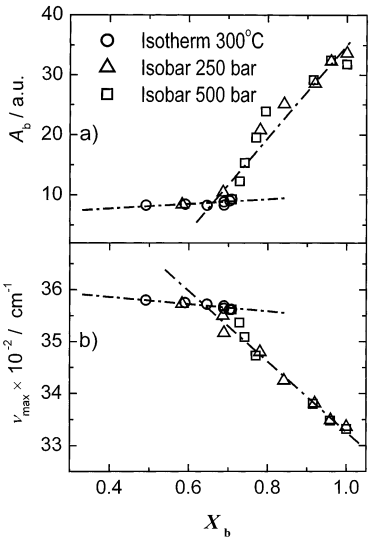

Figure 13. Correlation between the coefficient of integrated absorption A_b (circles), peak positions (triangles), and the mole fraction X_b of H-bonded OH groups in EtOH.

deconvolution with any known distribution function. The rotational branches in the spectrum of EtOH can be observed up to a pressure of at least 150−200 bar. At higher pressures, they are suppressed due to the increasing probability of collisions. The high-pressure spectra could be used in the same way as for ^{n}BuOH because we can recognize the presence of monomeric OH groups as a shoulder on the high-frequency side of the band. It is clear, however, that the extrapolation of I_{nb} to zero pressure could only give very uncertain results. It seems that the high-frequency feature in the spectra of MeOH in Figure 10 is resolved much better but, comparing the spectra of MeOH obtained in this work with the spectrum of MeOH in the gas phase indicates that this feature cannot be treated as the maximum of monomeric band. The peak position for the monomer cannot be higher than that of the Q branch of the gaseous spectrum. Evidently, it is the maximum of the R-rotational branch that is resolved. Moreover, there are no spectral manifestations of monomers in the remaining part of the contour. It is impossible, therefore, to find the intensity of non-H-bonded MeOH molecules with our deconvolution procedure.

All the same, there is a way to estimate roughly the extent of hydrogen bonding in scEtOH. First, we extrapolate the *total integrated intensity* of the OH band in the normalized spectra to zero pressure, as shown in Figure 12a. This again gives us the reduced coefficient of integrated absorption A_{nb} because at zero density there cannot be a contribution from H-bonded OH groups. Applying then the curve fitting procedure to the spectra obtained at pressures higher than 150 bar (not noticeably complicated by rotational transitions), we find I_{nb} and then the probability of hydrogen bonding X_b as $1 - I_{nb}/A_{nb}$. The accuracy of the estimate is, of course, rather low, but the behavior of X_b as a function of pressure (Figure 12b) reproduced surprisingly well the behavior of X_b for ^{n}BuOH and ^{i}PrOH. Figure 13 shows that the correlations between X_b and the parameters A_b, and ν_{max} are also much the same with breaking points at $X_b \approx 0.65$. This also suggests that at 350 °C scEtOH may exist mainly as a mixture of H-bonded dimers and monomers. Again, it is worth mentioning the comparison between the approximate position of ν_{max}, ca. 3580 cm^{-1} for the EtOH dimer, with that observed in the gas phase at ambient temperature (3570 cm^{-1})[69] and in the solution of ethanol in hexane[68] (3540 cm^{-1}).

5. Conclusion

It is difficult to make direct comparisons between the results presented here and previous investigations of sc alcohols. Earlier studies have concentrated almost entirely on scMeOH, and data on the higher alcohols are very scarce. Hoffmann and Conradi[38] showed that there are strong similarities between the behavior of the hydrogen bonding in water, MeOH, and EtOH when the results are expressed in terms of their reduced thermodynamic variables. Here, we find that trends in the results for ^{n}BuOH, ^{i}PrOH, and possibly EtOH are also similar. This suggests that the nature of hydrogen bonding across a whole series of alcohols may be more consistent than one would initially anticipate. Further work is required so that these findings can be tested.

In this work, an attempt has been made to characterize semiquantitatively the hydrogen bonding in a number of simple alcohols over a wide range of temperature and pressure, using an approach to the problem. The novelty of the approach lies in the method for obtaining the absorption coefficient for nonbonded OH groups when density data and path lengths in a HTHP cell are not available The approach could be used for other organic substances with O−H groups, other alcohols for example, but certain reservations should be kept in mind.

It is rather difficult to estimate to what degree uncertainty of the curve fitting procedure affects the above results. Taking into account all the factors mentioned, we can estimate the probable error in X_b to be ± 0.05 for ^{n}BuOH and ^{i}PrOH, whereas for EtOH it not less than ± 0.1.

The method is rather difficult to use for small molecules, when the spectrum of stretching vibrations is complicated by the rotational transitions, as in the case of MeOH and EtOH.

However, recently we have obtained independent confirmation of the fact that all alcohols, including MeOH, should behave very similarly with changing temperature and pressure. MD simulations of MeOH under a variety of external conditions, carried out by M. Kiselev,[74] have shown how the average energy of hydrogen bonding (E_{HB}) correlates with the mole fraction of H-bonded OH groups. The results of these MD calculations will be published in full but the conclusions are presented in Figure 14. One can see that the correlation between E_{HB} and X_b is exactly the same as for other alcohols studied. Even the bend of the function is observed at $X_b \approx 0.7$ as for the other alcohols explored in this work.

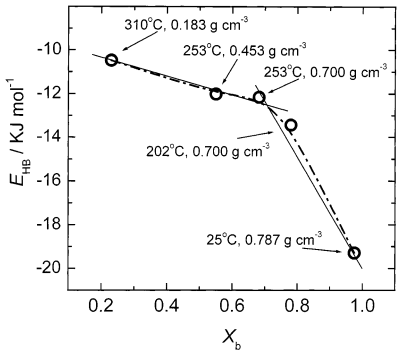

Figure 14. Correlation between the energy of hydrogen bonding and X_b for methanol. Courtesy of Dr. M. Kiselev.

The possibility of forming C−H···O hydrogen bonds has not been taken into consideration in this work. Such bonds, however, are by an order of magnitude weaker than O−H···O bonds and their influence might be unnoticed at the level of approximation used here.

The main results of our study are the pressure and temperature dependencies of the extent of hydrogen bonding for ^{n}BuOH and ^{i}PrOH. Studying the correlation between the integrated intensity of the absorption, the position of the band maximum, and the probability of hydrogen bonding, we arrived at the conclusion that mostly H-bonded dimers and monomers exist under supercritical conditions. The same but less reliable inference can be drawn from the spectra of scEtOH. The larger H-bonded complexes begin to form at the probability of H-bonding higher than 0.6−0.7 and this seems to be a general rule for all alkanols. Perhaps, such a threshold can be found in other systems with hydrogen bonds. The forming of the large H-bonded complexes (chains or rings) leads to the strengthening of hydrogen bonds due to *the cooperativity effect*, the first time that the effect has been demonstrated so explicitly.

Acknowledgment. We are grateful to Professor Y. Marcus and Dr. M. Rozenberg for useful comments and Dr. M. Kiselev for presenting his new data. The support from the Royal Society, the Russian Basic Research Foundation (Grant 00-05-64392), and the EPSRC (Grant GR/N06892) is greatly appreciated. We thank Mr. D. Merrifield and Mr. C. Valder for their help and Glaxosmithkline PLC for financial support. The technical assistance of Mr. M. Dellar and Mr. M. Guyler is greatly appreciated.

References and Notes

(1) Gude, M.; Teja, A. S. *J. Chem. Eng. Data* **1995**, *40*, 1025.
(2) Jessop, P. G., Leitner, W., Eds. *Chemical Synthesis Using Supercritical Fluids*; Wiley-VCH: Weinheim, 1999.
(3) Darr, J. A.; Poliakoff, M. *Chem. Rev.* **1999**, *99*, 495.
(4) Shaw, R. W.; Brill, T. B.; Clifford, A. A.; Eckert, C. A.; Franck, E. U. *Chem. Eng. News* **1991**, *69*, 26.
(5) Barj, M.; Bocquet, J. F.; Chhor, K.; Pommier, C. *J. Mater. Sci.*, **1992**, *27*, 2187.
(6) Bocquet, J. F.; Chhor, K.; Pommier, C. *Surf. Coat. Technol.* **1994**, *70*, 73.
(7) Yin, S.; Sato, T. *Ind. Eng. Chem. Res.* **2000**, *39*, 4526.
(8) Sako, T.; Sugeta, T.; Otake, K.; Nakazawa, N.; Sato, M.; Namiki, K.; Tsugumi, M. *J. Chem. Eng. Jpn.* **1997**, *30*, 342.
(9) Saka, S.; Kusdiana, D. *Fuel* **2001**, *80*, 225.
(10) Gubin, S. P. *Dokl. Akad. Nauk.* **1995**, *345*, 490.
(11) Pimentel, G. C.; McClellan, A. L. *The Hydrogen Bond*; Freeman: London, 1960.
(12) Jorgensen, W. L. *J. Phys. Chem.* **1986**, *90*, 1276.
(13) Chelli, R.; Ciabatti, S.; Cardini, G.; Righini, R.; Procacci, P. *J. Chem. Phys.* **1999**, *111*, 4218.
(14) Saiz, L.; Padro, J. A.; Guardia, E. *J. Phys. Chem. B* **1997**, *101*, 78.
(15) Saiz, L.; Guardia, E.; Padro, J. A. *J. Chem. Phys.* **2000**, *113*, 2814.
(16) Marti, J.; Padro, J. A.; Guardia, E. *J. Mol. Liq.* **1995**, *64*, 1.
(17) Gao, J. L.; Habibollazadeh, D.; Shao, L. *J. Phys. Chem.* **1995**, *99*, 16460.
(18) Wallen, S. L.; Palmer, B. J.; Garrett, B. C.; Yonker, C. R. *J. Phys. Chem.* **1996**, *100*, 3959.
(19) Narten, A. H.; Habenschuss, A. *J. Chem. Phys.* **1984**, *80*, 3387.
(20) Vahvaselka, K. S.; Serimaa, R.; Torkkeli, M. *J. Appl. Crystallogr.* **1995**, *28*, 189.
(21) Sarkar, S.; Joarder, R. N. *J. Chem. Phys.* **1993**, *99*, 2032.
(22) Sarkar, S.; Joarder, R. N. *J. Chem. Phys.* **1994**, *100*, 5118.
(23) Zetterstrom, P.; Dahlborg, U.; Howells, W. S. *Mol. Phys.* **1994**, *81*, 1187.
(24) Yamaguchi, T.; Hidaka, K.; Soper, A. K. *Mol. Phys.* **1999**, *96*, 1159.
(25) Yamaguchi, T.; Hidaka, K.; Soper, A. K. *Mol. Phys.* **1999**, *97*, 603.
(26) Benmore, C. J.; Loh, Y. L. *J. Chem. Phys.* **2000**, *112*, 5877.
(27) Weitkamp, T.; Neuefeind, J.; Fischer, H. E.; Zeidler, M. D. *Mol. Phys.* **2000**, *98*, 125.
(28) Bowron, D. T.; Finney, J. L.; Soper, A. K. *Mol. Phys.* **1998**, *93*, 531.
(29) Kusalik, P. G.; Lyubartsev, A. P.; Bergman, D. L.; Laaksonen, A. *J. Phys. Chem. B* **2000**, *104*, 9526.
(30) Yonker, C. R.; Wallen, S. L.; Palmer, B. J.; Garrett, B. C. *J. Phys. Chem. A* **1997**, *101*, 9564.
(31) Fulton, J. L.; Yee, G. G.; Smith, R. D. *J. Am. Chem. Soc.* **1991**, *113*, 8327.
(32) Kazarian, S. G.; Gupta, R. B.; Clarke, M. J.; Johnston, K. P.; Poliakoff, M. *J. Am. Chem. Soc.* **1993**, *115*, 11099.
(33) Kazarian, S. G.; Howdle, S. M.; Poliakoff, M. *Angew. Chem., Int. Ed. Engl.* **1995**, *34*, 1275.
(34) Gorbaty, Y. E.; Gupta, R. B. *Ind. Eng. Chem. Res.* **1998**, *37*, 3026.
(35) Kalinichev, A. G.; Bass, J. D. *Chem. Phys. Lett.* **1994**, *231*, 301.
(36) Mountain, R. D. *J. Chem. Phys.* **1989**, *90*, 1866.
(37) Hoffmann, M. M.; Conradi, M. S. *J. Am. Chem. Soc.* **1997**, *119*, 3811.
(38) Hoffmann, M. M.; Conradi, M. S. *J. Phys. Chem. B* **1998**, *102*, 263.
(39) Asahi, N.; Nakamura, Y. *Chem. Phys. Lett.* **1998**, *290*, 63.
(40) Asahi, N.; Nakamura, Y. *J. Chem. Phys.* **1998**, *109*, 9879.
(41) Bai, S.; Yonker, C. R. *J. Phys. Chem. A* **1998**, *102*, 8641.
(42) Tsukahara, T.; Harada, M.; Ikeda, Y.; Tomiyasu, H. *Chem. Lett.* **2000**, 420.
(43) Chalaris, M.; Samios, J. *J. Phys. Chem. B* **1999**, *103*, 1161.
(44) Yamaguchi, T.; Benmore, C. J.; Soper, A. K. *J. Chem. Phys.* **2000**, *112*, 8976.
(45) Ohno, K.; Yoshida, H.; Watanabe, H.; Fujita, T.; Matsuura, H. *J. Phys. Chem.* **1994**, *98*, 6924.
(46) Luck, W. A. P.; Fritzsche, M. *Z. Phys. Chem.* **1995**, *191*, 71.
(47) Dixon, J. R.; George, W. O.; Hossain, M. F.; Lewis, R.; Price, J. M. *J. Chem. Soc., Faraday Trans.* **1997**, *93*, 3611.
(48) George, W. O.; Has, T.; Hossain, M. F.; Jones, B. F.; Lewis, R. *J. Chem. Soc., Faraday Trans.* **1998**, *94*, 2701.
(49) Iwahashi, M.; Suzuki, M.; Katayama, N.; Matsuzawa, H.; Czarnecki, M. A.; Ozaki, Y.; Wakisaka, A. *Appl. Spectrosc.* **2000**, *54*, 268.
(50) Provencal, R. A.; Paul, J. B.; Roth, K.; Chapo, C.; Casaes, R. N.; Saykally, R. J.; Tschumper, G. S.; Schaefer, H. F. *J. Chem. Phys.* **1999**, *110*, 4258.
(51) Provencal, R. A.; Casaes, R. N.; Roth, K.; Paul, J. B.; Chapo, C. N.; Saykally, R. J.; Tschumper, G. S.; Schaefer, H. F. *J. Phys. Chem. A* **2000**, *104*, 1423.
(52) Haber, T.; Schmitt, U.; Suhm, M. A. *Phys. Chem. Chem. Phys.* **1999**, *1*, 5573.
(53) Schaal, H.; Haber, T.; Suhm, M. A. *J. Phys. Chem. A* **2000**, *104*, 265.
(54) Zimmermann, D.; Haber, T.; Schaal, H.; Suhm, M. A. *Mol. Phys.* **2001**, *99*, 413.
(55) Buck, U.; Huisken, F. *Chem. Rev.* **2000**, *100*, 3863.
(56) Luck, W. A. P.; Ditter, W. *Ber. Bunsen-Ges. Phys. Chem.* **1968**, *72*, 365.
(57) Ebukuro, T.; Takami, A.; Oshima, Y.; Koda, S. *J. Supercrit. Fluids* **1999**, *15*, 73.
(58) (a) Gorbaty, Y. E.; Bondarenko, G. V. *Appl. Spectrosc.* **1999**, *53*, 908. (b) We have recently reviewed the different types of cell that can be used for such experiments, explaining the relative advantages of fixed and variable path length cells: Barlow, S. J.; George M. W.; Poliakoff, M. Vibrational Spectroscopy and Supercritical Fluids. In *Handbook of Vibrational Spectroscopy*; Chalmers J. M., Griffiths P. R., Eds.; John Wiley & Sons Ltd.: New York, 2002; Vol. 4, p 3124.
(59) Huisken, F.; Kaloudis, M.; Koch, M.; Werhahn, O. *J. Chem. Phys.* **1996**, *105*, 8965.
(60) Gupta, R. B.; Brinkley, R. L. *AIChE J.* **1998**, *44*, 207.
(61) Førland, G. M.; Liang, Y. Kvalheim, O. M.; Høiland, H.; Chazy, A. *J. Phys. Chem. B* **1997**, *101*, 6960.
(62) Walsh, J. M.; Donohue, M. D. *Fluid Phase Equilib.* **1989**, *52*, 397.

(63) Economou, I. G.; Donohue, M. D. *AIChE J.* **1991**, *37*, 1875.
(64) Fulton, J. L.; Yee, G. G.; Smith, R. D. *J Supercrit. Fluids* **1990**, *3*, 169.
(65) Iogansen, A. V. *Spectrochim. Acta* **1999**, *A55*, 1585.
(66) Iogansen, A. V.; Rozenberg, M. Sh. *Opt. Spectrosc.* **1978**, *44*, 49 (in Russian).
(67) Gorbaty, Y. E.; Kalinichev, A. G. *J. Phys. Chem.* **1995**, *99*, 5336.
(68) Asprion, N., Hasse, H., Maurer, G. *Fluid Phase Equilib.* **2001**, *186*, 1.
(69) Barnes, A. J.; Hallam, H. E.; Jones, D. *Proc. R. Soc. London* **1973**, *335*, 97.
(70) Veytsman, B. A. *J. Phys. Chem.* **1993**, *97*, 7144.
(71) Sear, R. P.; Jackson, G. *J. Chem. Phys.* **1996**, *105*, 1113.
(72) Gorbaty, Y. E.; Bondarenko, G. V.; Kalinichev, A. G.; Okhulkov, A. V. *Mol. Phys.* **1999**, *96*, 1659.
(73) Yukhnevich, G. V. *Spectrosc. Lett.* **1997**, *30*, 901.
(74) Kiselev, M. Private communication, unpublished data.
(75) NIST Database, http://webbook.nist.gov/chemistry/name-ser.html Thermo Galactic Spectra On-line. http://spectra.galactic.com/SpectraOnline/Default_ie.htm.